A new methodology for estimating field horizontal stress from microseismic focal mechanisms

Alireza Agharazi[1*], Peter Duncan[1] and Michael Thornton[1] introduce a new methodology for the estimation of field σ_{Hmax} magnitude and direction from microseismic focal mechanisms.

Introduction

The full stress state in a formation is characterized by the directions and magnitudes of the three principal stresses. It is common practice to take the vertical stress, σ_v, and the minimum and maximum horizontal stresses, σ_{hmin} and σ_{Hmax}, as the principal stresses in unconventional reservoirs. Considering the relatively high depth of most unconventional reservoirs, which results in a very high vertical stress magnitude, this assumption holds true in most cases unless a geological feature such as a fault or fold changes the stresses locally. The magnitude of vertical stress can easily be determined by integrating the density of overburden rocks from density logs. A good estimate of σ_{hmin} magnitude can be obtained from well test results such as a mini-frac test or a diagnostic fracture injection test. The magnitude of σ_{Hmax}, however, remains the most challenging stress component to determine.

Wellbore breakout analysis is the most common method for determining σ_{Hmax} magnitude at the depths of unconventionals. (Zoback, 2010). A main limitation of this method is that it cannot be applied where no breakout occurs around the monitor well. In many cases the field deviatoric stresses are not high enough, with respect to rock strength, to cause any failure around a wellbore.

The stress inversion technique, frequently used by seismologists to estimate the stresses governing earthquake focal mechanisms, has also been used by some authors to determine the formation stresses for unconventional reservoirs from microseismic focal mechanisms (Neuhaus et al., 2012; Sasaki and Kaieda 2002; Stanek et al., 2015). A fundamental assumption in this technique is that all focal mechanisms follow the same stress model, (Sasaki and Kaieda, 2002) so a best-fit solution can be found that represents the field stresses. However, this assumption is not often valid in the case of microseismic focal mechanisms acquired during hydraulic fracturing stimulations in naturally fractured reservoirs, mainly owing to local stresses developed by the interaction of natural fractures.

In this paper, we introduce a new methodology for the estimation of field σ_{Hmax} magnitude and direction from microseismic focal mechanisms. In this new method, the direction of horizontal stresses are first determined by searching for the focal mechanisms that are aligned with horizontal stresses, using a geometric criterion. Having determined the σ_{Hmax} direction, a linear relationship is established between the magnitudes of minimum and maximum horizontal stresses normalized by the magnitude of vertical stress. Provided that the minimum and vertical stresses are known, the magnitude of the maximum horizontal stress can be determined for each qualified microseismic focal mechanism. The field σ_{Hmax} magnitude is then determined by statistical analysis of all calculated σ_{Hmax} magnitudes.

The key to the success of the proposed method is the identification of the qualified focal mechanisms for stress estimation. These are identified using a mathematical algorithm that assesses each focal mechanism individually and tags it by the stress model that is consistent with the focal mechanism. Three verification examples, using numerical simulation results, and three case studies, using real data from the Marcellus shale, are provided. A brief discussion on the impact of σ_{Hmax} magnitude on the completion design parameters and efficiency follows the case studies.

Seismic moment tensor and focal mechanism

The inputs to the stress analysis are the microseismic focal mechanisms recorded during a hydraulic fracturing treatment. The focal mechanism is derived from the seismic moment tensor that is established for each event. The seismic moment tensor is a second-order tensor that describes the deformation mechanisms in the immediate vicinity of a seismic source. It characterizes the seismic event magnitude, fracture type (e.g., shear, tensile), and fracture orientation. A moment tensor inversion technique is invoked to establish the moment tensor for each event by

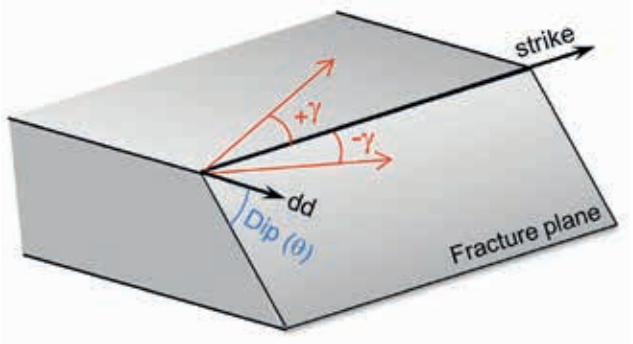

Figure 1 Schematic picture shows fault plane solution (failure plane dip and strike) and slip direction (rake angle). The strike is measured clockwise from north, ranging from 0° to 360°, with the fracture plane dipping to the right when looking along the strike direction. The dip is measured from horizontal and varies from 0° to 90°. The slip (or rake) vector represents the slip direction of hanging wall relative to foot wall. The rake angle is the angle between the strike direction and the rake vector. It changes from 0° to 180° when measured counterclockwise from strike and from 0° to –180° when measured clockwise from strike (when viewed from the hanging wall side).

[1] MicroSeismic, Houston, Texas, USA
* Corresponding author, E-mail: aagharazi@microseismic.com

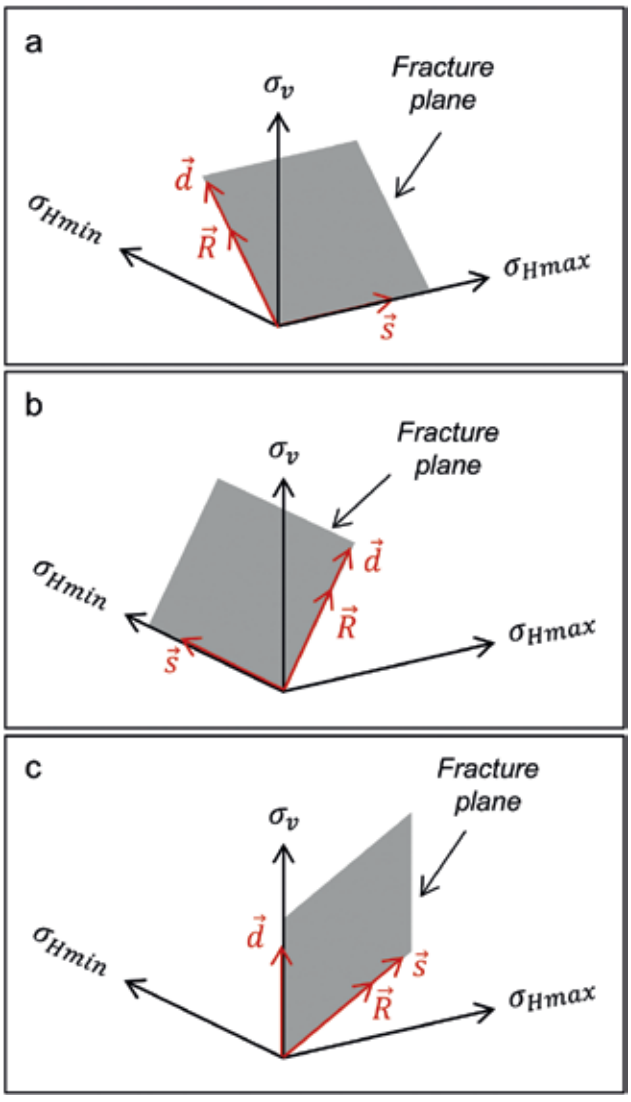

Figure 2 Fracture planes with dip or strike parallel to one of the principal stresses. These fractures cannot be used for stress calculations because their rake vector (**R**) is no longer a function of relative stress magnitudes. The non-vertical fractures with their strike parallel to one of the horizontal stresses (Image a and Image b) show a pure dip-slip mechanism and can be used to determine the direction of horizontal stresses.

minimizing a residual function, usually a least-squares function, for all wave patterns recorded for a given event by different receivers. Details of moment tensor inversion techniques can be found in Jost and Herrmann (1989) and Dahm and Kruger (2014).

The source mechanism parameters such as fracture orientation and slip direction (Figure 1) is determined from the eigenvectors and eigenvalues of the moment tensor (Jost and Herrmann, 1989). The fault plane solution that results from this approach comes with an inherent ambiguity in the fracture orientation, in that it produces two theoretically possible failure planes – a real and an auxiliary plane that are orthogonal to each other. The auxiliary plane has no physical meaning and is merely the byproduct of the solution. The moment tensor itself does not provide any further information that can be used to distinguish the real plane (Cronin, 2010).

Another potential problem in the fault plane solution is the polarity in the rake vector. Since the moment tensor is estimated from noisy data, near-vertical slip planes can become problematic. Slight deviations of the estimated dip of the slip plane on either

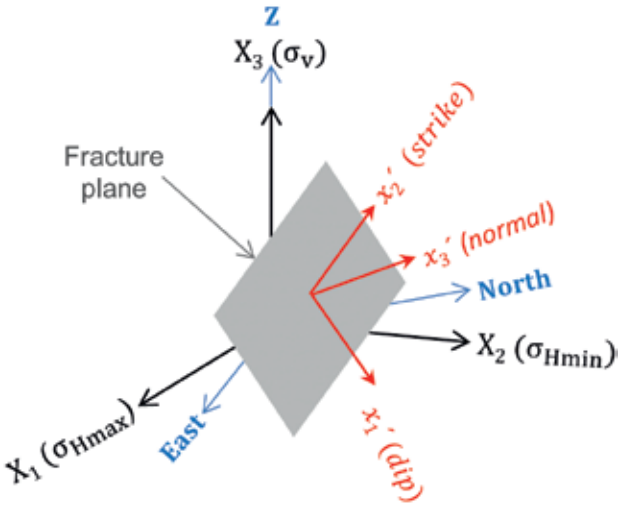

Figure 3 Geographic coordinate system E-N-Z (blue), reference (principal stresses) coordinate system σ_{Hmax} -σ_{hmin} -σ_v (black), and fracture local coordinate system dip-normal-strike (red).

side of vertical can produce an artificially reversed rake vector for some events, meaning that the calculated slip direction is 180° off from the real slip direction. These two issues must be taken into account and properly addressed when using microseismic focal mechanisms for field stress estimation.

Stress calculation method

The stress calculation includes three main steps: i) determination of horizontal stress direction and forming the reference coordinate system, ii) pre-processing of focal mechanisms to find qualified events for stress calculation, and iii) the calculation of maximum horizontal stress magnitude.

Consistent with common practice in the industry, the vertical stress is assumed as a principal stress, implying that the other two principal stresses are horizontal. Provided there are no major structural features, such as a fold or a fault, this assumption is generally valid for most unconventional reservoirs.

Assuming the vertical stress is a principal stress, the direction of horizontal stresses can be determined from the focal mechanisms that meet a certain geometric criterion. In a field where the vertical stress is a principal stress, the shear stress projection on any non-vertical fracture plane that is parallel to one of the horizontal stresses makes a right angle with the fracture strike (Figure 2a and 2b). This is because the stress component that is parallel with the fracture plane strike has no projection on the plane, resulting in a shear stress projection perpendicular to the strike. Assuming rake and shear stress vectors are parallel, the focal mechanisms with the rake angle of ±90° can be picked and used to estimate the horizontal stress directions.

Having determined the direction of horizontal stresses, the reference coordinate system is formed as a right-handed coordinate system with σ_{Hmax}, σ_{hmin}, and σ_v directions being the first (X_1), second (X_2), and third (X_3) coordinate axes, respectively (Figure 3).

The calculation of σ_{Hmax} magnitude from microseismic focal mechanisms is based on the assumption that when rock fails in shear it slips in the direction of maximum shear stress acting on the failure plane. Therefore, if the orientation of the failure plane and slip direction on the plane is known, it is possible to

back-calculate the stresses governing the failure and post-failure slip. This condition is mathematically represented by:

$$\boldsymbol{R} \times \boldsymbol{T_s} = 0 \tag{1}$$

where ($\boldsymbol{R}$) is the rake vector and ($\boldsymbol{T_s}$) is the shear projection of stresses on the failure plane. It should be noted that Eq. 1 remains valid as long as the two vectors are parallel, regardless of their direction. This eliminates any potential error caused by the polarity issue that might exist in some focal mechanisms, as discussed previously.

The rake vector ($\boldsymbol{R}$) is written in the reference coordinate system as follows: (Agharazi, 2016):

$$\boldsymbol{R} = R_1\boldsymbol{X_1} + R_2\boldsymbol{X_2} + R_3\boldsymbol{X_3} \tag{2}$$

$$\mathrm{R}_1 = -\sin\gamma\cos\theta\sin\beta + \cos\gamma\sin\alpha \tag{3}$$

$$R_2 = -\sin\gamma\cos\theta\cos\beta + \cos\gamma\cos\alpha \tag{4}$$

$$R_3 = \sin\gamma\sin\theta \tag{5}$$

where γ is the rake angle (Figure 1), α is the fracture strike angle measured from σ_{hmin} (X_2 axis in the reference coordinate system), θ is the fracture dip angle measured from horizontal, and α is the dip direction angle (ß = a + 90). The components of the rake vector ($\boldsymbol{R}$) are solely functions of the microseismic event focal mechanism and are derived from the seismic moment tensor.

The stress tensor is represented by a diagonal matrix in the reference coordinate system as follows:

$$\sigma_{ij} = \begin{bmatrix} \sigma_{11} & 0 & 0 \\ 0 & \sigma_{22} & 0 \\ 0 & 0 & \sigma_{33} \end{bmatrix} = \begin{bmatrix} \sigma_{Hmax} & 0 & 0 \\ 0 & \sigma_{hmin} & 0 \\ 0 & 0 & \sigma_v \end{bmatrix} \tag{6}$$

Considering the vertical scatter of induced microseismic events, the components of the stress tensor must be normalized by a depth factor. Assuming vertical stress is defined as $\sigma_v = d \times \sigma_{vGrad}$ where d is depth and σ_{vGrad} is vertical stress gradient, with units of stress over length such as MPa/m, the stress tensor can be normalized by vertical stress as follows:

$$S_{ij} = \frac{\sigma_{ij}}{\sigma_v} = \begin{bmatrix} k_H & 0 & 0 \\ 0 & k_h & 0 \\ 0 & 0 & 1 \end{bmatrix} \tag{7}$$

where:

$$k_H = \sigma_{Hmax}/\sigma_v$$
$$k_h = \sigma_{hmin}/\sigma_v$$

An important advantage of normalizing the stress tensor by vertical stress is that it eliminates the vertical stress component from future equations, leaving k_H and k_h as the only variables.

The components of the shear stress vector ($\boldsymbol{T_s}$) acting on a failure plane with normal vector $\boldsymbol{n}$ can be determined in the reference coordinate system as follows (Agharazi, 2016):

$$\boldsymbol{T_s} = T_{s1}\boldsymbol{X_1} + T_{s2}\boldsymbol{X_2} + T_{s3}\boldsymbol{X_3} \tag{8}$$

$$T_{s1} = \sigma_v N_1\left[N_2{}^2(k_H - k_h) - N_3{}^2(1 - k_H)\right] \tag{9}$$

$$T_{s2} = \sigma_v N_2\left[N_3{}^2(k_h - 1) - N_1{}^2(k_H - k_h)\right] \tag{10}$$

$$T_{s3} = \sigma_v N_3\left[N_1{}^2(1 - k_H) - N_2{}^2(k_h - 1)\right] \tag{11}$$

where N_1, N_2 and N_3 are the components of the failure plane normal vector $\boldsymbol{n}$ in the reference coordinates, which are known from the fault plane solution.

Substituting rake and shear vectors from Equation 2 and Equation 8 in Eq. 1, the following linear relationship is obtained between k_H and k_h:

$$k_H = M_1 + M_2 k_h \tag{12}$$

The coefficients M_1 and M_2 in Eq. 12 are solely functions of rake vector and fracture orientation and can be calculated from the following equations:

$$M_1 = a_3/a_1 \tag{13}$$

$$M_2 = a_2/a_1 \tag{14}$$

where:

$$a_1 = R_3N_2N_1{}^2 - R_2N_3N_1{}^2 \tag{15}$$

$$a_2 = R_2N_3N_2{}^2 + R_3N_2N_3{}^2 + R_3N_2N_1{}^2 \tag{16}$$

$$a_3 = -R_2N_3N_1{}^2 - R_2N_3N_2{}^2 - R_3N_2N_3{}^2 \tag{17}$$

More details on derivation of these equations can be found in Agharazi (2016).

Eq. 12 establishes a linear relationship between the normalized magnitudes of σ_{Hmax} and σ_{hmin}. Provided that the magnitudes of σ_{hmin} and σ_v are known (for example, from a mini-frac test and density logs, respectively), k_H and the absolute magnitude of σ_{Hmax} can be calculated for each focal mechanism. In this methodology, each microseismic event is considered as an independent field test. The field σ_{Hmax} can then be determined by statistical analysis of calculated σ_{Hmax} values for all qualifying focal mechanisms.

Challenges and solution

The main challenge in estimating stresses from microseismic focal mechanisms is how to identify the events that are compatible with the dominant field stress regime so that they can be used to back-calculate field stresses. These events are mainly associated with the shear failures that are triggered by the build-up of fluid pressure under undisturbed field stresses. In most microseismic data sets, there are events whose focal mechanism is not compatible with the dominant field stress regime. The incompatible focal mechanisms must be identified and excluded from stress analysis, or otherwise a significant error occurs in the calculated stress magnitudes. The main factors causing incompatibility of focal mechanisms with the field stress regime are:

- Stress disturbances caused by hydraulic fracture propagation in the formation. Numerical studies show that the propagation of a

hydraulic fracture results in two distinct stress-modified zones; i) a shear zone at the propagating tip of the fracture with rotated stresses and ii) a compressive zone (stress shadow zone) on either side of the open fracture with increased stress magnitudes (Agharazi et al., 2013). The focal mechanisms located in these zones are not representative of initial field stresses.

- Local stress changes resulting from the interaction of natural and hydraulic fractures in naturally fractured reservoirs. Stress relaxation and concentration at the intersection of active fractures (slipping or opening) results in local stresses that are different from field stresses either in magnitude or direction. The focal mechanisms associated with these stresses are not compatible with the initial field stresses.
- Ambiguity in fault plane solution. This results in inconsistent events with field stress configuration.
- Error in fault plane solution. The inversion technique used to determine the seismic moment tensor for each event provides the best-fit model based on the observed waveforms. Hence, the solution comes with a level of uncertainty that is distributed to the fault plane solution parameters, i.e., failure plane orientation and slip direction. The uncertainty level depends on several factors, among which the signal-to-noise ratio (SNR) is of the most importance. A high level of error in fault plane solution parameters might result in inconsistent focal mechanisms with the overall field stress regime.

The proportion of incompatible events in a microseismic data set depends on various factors, such as density and orientation of natural fractures, overall noise level relative to signal strength, and accuracy of moment tensor inversion.

The incompatible events can be identified mathematically by establishing Eq. 12 for each focal mechanism. The coefficients M_1 and M_2 follow a sign convention consistent with the field stress regime that governs the slip on the failure plane, as shown in Table 1. The incompatible events can be idientified if a general knowledge of field stress regime (i.e., normal faulting, strike-slip, reverse faulting) is available. For example, in a normal faulting stress regime, where $\sigma_{hmin} < \sigma_{Hmax} < \sigma_v$ (or $k_h < k_H < 1$), both coefficients must be positive for a focal mechanism to be considered compatible. Any focal mechanism with negative M_1 or M_2 is considered incompatible with the field stress and is excluded from the stress analysis.

After tagging all events with their corresponding stress regime, the field σ_{Hmax} is estimated from the events whose focal mechanisms follow the field stress regime. The undisturbed is determined by the statistical analysis of valid results, such as least-squares best-fitting for the known field.

Stress regime	Stress State	Normalized stresses	M_1	M_2
Normal Faulting	$\sigma_{hmin} < \sigma_{Hmax} < \sigma_v$	$k_h < k_H < 1$	+	+
Strike-slip	$\sigma_{hmin} < \sigma_v < \sigma_{Hmax}$	$k_h < 1 < k_H$	+	–
Reverse Faulting	$\sigma_v < \sigma_{hmin} < \sigma_{Hmax}$	$1 < k_h < k_H$	–	+

Table 1 Signs of M1 and M2 for three possible stress regimes.

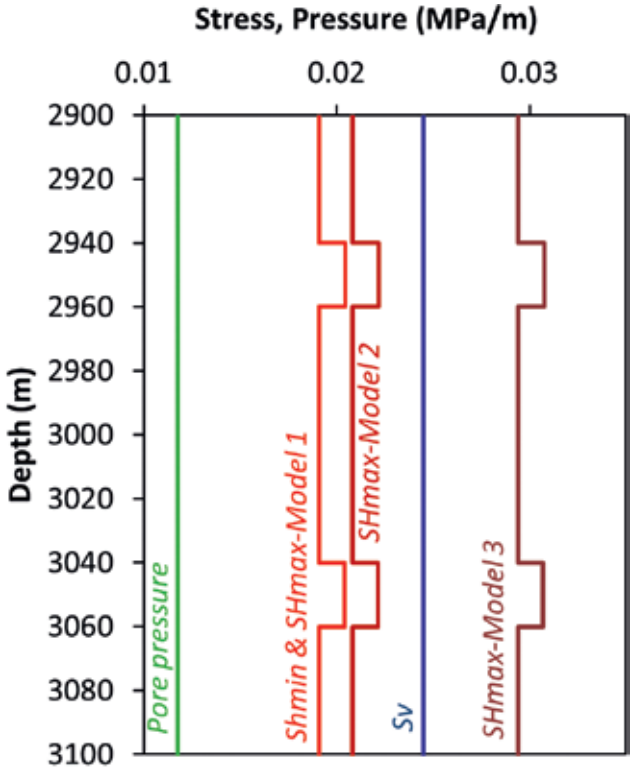

Figure 4 Stress profiles applied to numerical models. In Model 1, $\sigma_{Hmax} = \sigma_{hmin}$. The well depth is 3000 m.

Verification

We performed three numerical simulations of hydraulic fracturing in a naturally fractured reservoir. The objective was to back-calculate the applied σ_{Hmax} magnitude from the synthetic microseismic events collected during the simulations to verify the new methodology.

The model consisted of an 80-m thick pay zone confined by two stress barrier layers of 20-m thick at the top and bottom. The formation was intersected by two fracture sets oriented at 030º±2º/85º±2º and 110º±2º/85º±2º (dip direction/dip). One hour injection of slickwater (2.5 cP) at a pump rate of 60 barrels per minute was simulated. The synthetic microseismic events were constantly recorded during the simulation. For each synthetic event, the failure plane orientation and slip direction were recorded.

Three different stress models were examined – normal faulting in the first and second models, and strike-slip in the third model. In the first model σ_{Hmax} was set equal to σ_{hmin}, which replicates a case with zero horizontal stress anisotropy. In the second model a horizontal stress anisotropy was considered. In the third model σ_{Hmax} magnitude was raised such that the stress regime switched to a strike-slip model. Figure 4 shows the applied stress and pressure profiles to the three studied models. All other mechanical and completion parameters were kept similar in the three models.

The applied σ_{Hmax} magnitude was back-calculated for the three models using the suggested methodology in this paper. The results are shown in Table 2.

In all three cases, the back-calculated σ_{Hmax} magnitude perfectly match applied values, verifying the accuracy of the stress analysis methodology.

	Model 1	Model 2	Model 3
Stress Regime	Normal Faulting	Normal Faulting	Strike Slip
σ_v (MPa/m) (applied)	0.025	0.025	0.025
σ_{hmin} (MPa/m) (applied)	0.019	0.019	0.019
σ_{Hmax} (MPa/m) (applied)	0.019	0.021	0.029
No. of Synthetic MS events	19,923	13,127	16,310
No. of qualified events for stress calculation	7,863	12,021	14,319
$\sigma_{Hmax} - \sigma_{hmin}$ relationship	KH= 0.047+ 0.953kh	KH= 0.337+ 0.663kh	KH= 1.940- 0.940kh
Back-calculated σ_{Hmax} (MPa/m)	0.019	0.021	0.030

Table 2 Applied stresses to numerical models and back-calculated σ_{Hmax} values.

	Case A	Case B	Case C
No. of MS events >=SNR	1625	286	865
SNR	8	10	6
No. of qualified events	423	77	293
σ_v (MPa/m)	0.0265	0.0266	0.265
σ_{hmin} (MPa/m)	0.0181	0.0179	0.0181
$\sigma_{Hmax} - \sigma_{hmin}$ relationship	KH= 0.164+ 0.836kh	KH=0.144+ 0.856kh	KH= 0.129+ 0.871kh
Back-calculated σ_{Hmax} (MPa/m)	0.0195	0.0191	0.0192
Estimated σ_{Hmax} direction	N052	N57	N62
Stress regime	NF	NF	NF

Table 3 Stress analysis results for three case studies.

Case studies

We studied three cases from the Marcellus shale. In all cases, microseismic monitoring was carried out using surface arrays. A site-specific SNR threshold was applied in each case to filter out noisy data. The studied cases are located in the same region, less than 30 miles away from each other. All cases were treated using slickwater and the plug-and-perf method but by different pumping companies.

Case A includes three horizontal wells with an average lateral length of 1800-2100 m. The average stage length was 52 m. Each well was completed independently after the completion of the previous well. In total, 2409 microseismic events were recorded in the Marcellus layer. A minimum signal-to-noise ratio of SNR≥8 was applied.

Case B represents the first 760 m of two horizontal zipper-fracked wells, with a well spacing of approximately 490 m. In total, 286 microseismic events were recorded. The minimum SNR threshold was set to SNR=10.

Case C includes two horizontal wells completed independently, with an average lateral length of approximately 2100 m and average well distance of 460 m. In total, 1002 microseismic events were recorded in the Marcellus layer. The SNR threshold was set to SNR=6.

The vertical stress gradient was calculated from density logs for each case. The σ_{hmin} gradient was either reported by the operator or was taken from the available post job reports. The σ_{Hmax} was back-calculated from qualifying microseismic focal mechanisms. Table 3 shows the breakdown of microseismic events and the stress values. The back-calculated σ_{Hmax} magnitudes are within the same range, consistent with the proximity of the studied wells.

Discussion

Comparison with other methods

Wellbore breakout analysis: Similar to the methodology introduced in this paper, the wellbore breakout analysis also establishes a relationship between σ_{Hmax} and other field stresses. In either case, the σ_{Hmax} magnitude can be determined if the magnitude of the other two principal stresses are known. The application of the wellbore breakout analysis is, however, limited to cases where a breakout occurs under field stresses. In many cases the induced stress concentration around wellbore is not high enough to overcome rock strength and initiate a breakout. The other important factors affecting the accuracy of stress calculation using this method are:

- Failure criterion and rock strength parameters: An assumption must be made about the failure criterion governing the rock failure in the study formation. The corresponding rock strength parameters must also be determined. The rock strength parameters are usually major unknowns and can introduce a high level of uncertainty if not constrained precisely.
- Formation pressure: An accurate estimate of formation pressure must be available
- Scale effect: The estimated stress using this method is more representative of local stresses around the study well, which may or may not be equal to field stresses at large scale. A geological feature, such as a fault, can significantly disturb stresses locally around a well. This effect cannot be captured by the wellbore breakout analysis.

In comparison, the methodology introduced in this paper is independent of rock strength parameters and formation pressure, simply because its governing equation is solely based on the post-failure slip, irrespective of the mechanisms controlling the failure. The scale at which the stress is estimated varies from stage scale to pad scale, depending on the microseismic data set used as input for the analysis.

Stress inversion: In this method, a stress model, consisting of three principal stress directions and a ratio of the stress magnitudes, is sought that best fits the observed microseismic focal mechanisms. Several versions of this technique have been developed and published by different authors such as Michael (1984), Angelier (1990), Gephart and Forsyth (1984), Reches (1987). The main difference in these versions is the chosen residual function that is minimized during the inversion process. While successful application of this method were reported by several authors for the

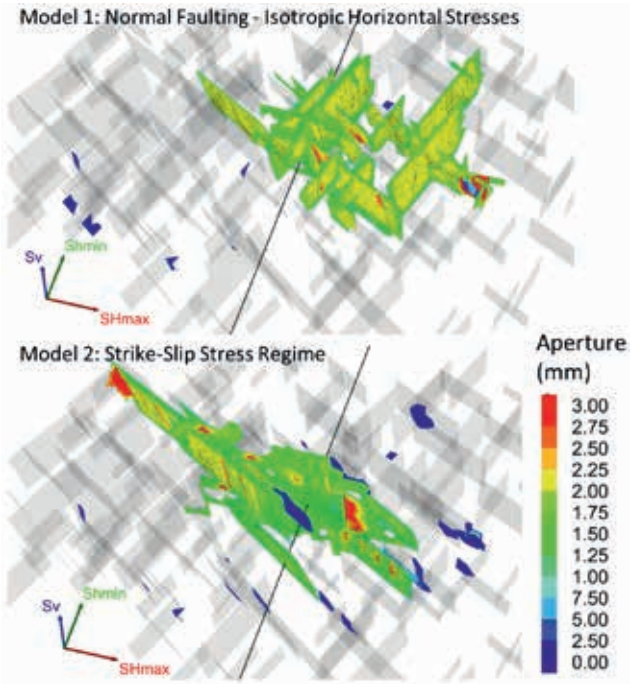

Figure 5 3D view of fracturing patterns after one hour of injection under two different horizontal stress magnitudes.

determiniation of stresses governing earthquake focal mechanisms (Michael, 1984; Gephart and Forsyth, 1984), it usually fails to produce consistent and representative results when applied to a large number of microseismic focal mechanisms recorded during a hydraulic fracturing stimulation. This is mainly because this method is unable to detect the incompatible and unqualified events that exist in the data set, resulting in back-calculating a single stress model for the focal mechanisms that follow different stress models. The divergence from the true field stress model increases with the increase in the ratio of incompatible events in the data set. This effect can be clearly seen when various subsets of a given microseismic data set are used for stress inversion (Stanek et al., 2015). To demonstrate this effect, we applied the stress inversion technique to estimate the stress model for the second case study (Case B) in the Marcellus. We used the stress inversion method suggested by Michael (1984) with a miss-fit angle threshold of 45º.

We applied the stress inversion on the focal mechanisms for each well separately. The same vertical and minimum horizontal stress magnitudes shown in Table 3 were used for both wells. The stress inversion technique resulted in two different stress regimes for these wells – a normal faulting stress regime for Well A with σ_{Hmax}=0.025 MPa/m ($<\sigma_v$ =0.0266 MPa/m) and a strike-slip stress regime for Well B with σ_{Hmax}=0.028 MPa/m ($>\sigma_v$ =0.0266 MPa/m). For the sake of comparison, we used the same data sets to calculate the magnitude for both wells using the suggested methodology in this paper. In this case a normal faulting stress regime with σ_{Hmax}=0.0193 MPa/m was calculated for both wells.

The inconsistency in the stress inversion results comes from the difference in the proportion of incompatible events in the data set for each well, which is 40% in well A and 80% in well B. It is important to note that when the method introduced in this paper is used, a similar σ_{Hmax} magnitude is obtained for both wells, irrespective of different ratios of incompatible events in each data set. The calculated σ_{Hmax} magnitude for either well is also equal to the one that was calculated using the focal mechanism from both wells combined as reported in Table 3.

The impact of σ_{Hmax} on completion design

In a homogeneous and isotropic rock with no discontinuities, an induced hydraulic fracture propagates along the σ_{Hmax} direction. In naturally fractured reservoirs, however, this is not usually the case. Hydraulic fracture propagation depends on the interaction of the propagating fracture with natural fractures, which to a large extent depends on the field stresses. In these cases, the deviatoric stress or stress anisotropy (difference between the magnitudes of principal stresses) has a significant impact on the final stimulation pattern. A high deviatoric stress promotes stimulation of natural fractures, shifting the stimulation pattern from a classic planar transverse fracture geometry to a more volumetric stimulation, dominated by the stimulation of natural fractures. This factor potentially affects the optimum stage length and well spacing for a given treatment plan. Figure 5 shows the final stimulation pattern for two of the numerical models discussed previously – the normal faulting stress model with no horizontal stress anisotropy and the stike-slip model.

As the plots show in Figure 5, in the first model with zero horizontal stress anisotropy, the stimulation pattern is mainly dominated by the stimulation of natural fractures versus propagation of a planar fracture along the σ_{Hmax} direction. Both natural fracture sets are affected by the injection, and the stimulated volume expands almost equally in either horizontal direction. By shifting to the strike-slip stress regime in the second model, the stimulation pattern becomes a combination of planar hydraulic fracture propagation along the direction and stimulation of more favourably oriented natural fractures with respect to the applied field stress directions. In this case, the stimulated volume tends to expand more along the σ_{Hmax} direction than along the well. No major stimulation of the second fracture set is observed in this case.

These numerical examples show the impact of relative stress magnitudes on the final stimulation pattern and, therefore, on optimum stage length and well spacing in naturally fractured reservoirs. Based on these examples, the combination of more

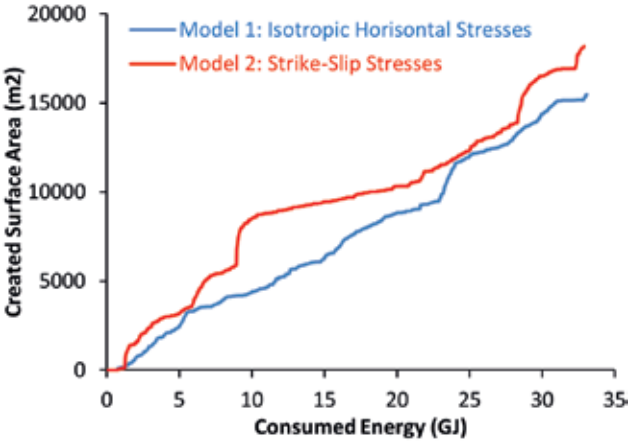

Figure 6 Created surface area versus consumed energy for two numerical simulations.

closely spaced wells with longer stages is likely more efficient in formations with zero or low stress anisotropy, whereas more widely spaced wells with shorter stage lengths are required for efficient stimulation in formations with high-stress anisotropy.

The relative magnitudes of principal stresses also impact the economic efficiency of a completion design. Figure 6 shows the created contact surface area versus consumed energy plots for the two studied models. As these graphs show, for an equal amount of consumed energy, after one hour of pumping, the model with higher stress anisotropy returned approximately 25% higher created surface area, suggesting it is cheaper to stimulate a formation with higher stress anisotropy.

While these conclusions are case specific, they still show the significant impact that relative stress magnitudes have on completion design and efficiency in naturally fractured reservoirs.

Conclusion

A new methodology was introduced for the estimation of maximum horizontal stress from microseismic focal mechanisms acquired during a hydraulic fracturing stimulation. The methodology was verified by back-calculating the maximum horizontal stress for three numerical models of a hydraulic fracturing treatment in a naturally fractured reservoir. Three different stress regimes were applied to the models and for each case the applied maximum horizontal stress was back calculated from the synthetic microseismic events collected during the simulations.

Three Marcellus case studies were provided. For each case the direction and magnitude of the maximum horizontal stress were back calculated from the microseismic focal mechanisms collected during the treatment. The back calculated stress magnitudes for the studied cases were approximately similar, which was expected considering the close proximity of the studied wells.

The advantages of the suggested method over two other stress analysis techniques, i.e. wellbore breakout analysis and stress inversion, were briefly discussed. A key step in the suggested methodology is identifying the focal mechanisms that are not compatible with the field stress regime, and excluding them from stress analysis. Combining the compatible and incompatible focal mechanisms is probabely the main reason for the failure of stress inversion techniques when applied to microseismic focal mechanisms acquired during hydraulic fracturing treatments. This problem was demonstrated by applying the stress inversion technique to a set of microseismic data from two Marcellus wells.

The impact of stress magnitudes on the completion parameters and stimulation pattern was also investigated by performing numerical simulations. It was demonstrated how the stimulation pattern and efficiency changed when the maximum horizontal stress magnitude varied.

References

Agharazi, A. [2016]. Determination of Maximum Horizontal Field Stress from Microseismic Focal Mechanisms – A Deterministic Approach. *50th U.S. Rock Mechanics/Geomechanics Symposium*, Abstracts.

Agharazi, A., Lee, B., Nagel, N.B., Zhang, F. and Sanchez, M. [2013]. Tip-Effect Microseismicity – Numerically Evaluating the Geomechanical Causes for Focal Mechanisms and Microseismicity Magnitude at the Tip of a Propagating Hydraulic Fracture. *SPE Unconventional Resources Conference*, Extended Abstracts.

Angelier, J. [1990]. Inversion of Field Data in Fault Tectonics to Obtain the Regional Stress, A New Rapid Direct Inversion Method by Analytical Means. *Geophysical Journal International,* **103**, 363–376.

Cronin, V. [2010]. *A Primer on Focal Mechanism Solutions for Geologists.* Science Education Resource Center, Carleton College, Northfield, USA.

Dahm, T. and Kruger, F. [2014]. Moment Tensor Inversion and Moment Tensor Interpretation. In: Bormann, P. (Ed.), *New Manual of Seismological Observatory Practice 2 (NMSOP-2)*, Deutsches GeoForschungsZentrum, Potsdam, Germany, 1–37.

Engelder, T., Lash, G.G. and Uzcategui, R.S. [2009]. Joint Sets that Enhance Production from Middle and Upper Devonian Gas Shales of the Appalachian Basin. *The American Association of Petroleum Geologists Bulletin,* **93** (7), 857–889.

Gephart, J.W. and Forsyth, D.W. [1984]. An Improved Method for Determining the Regional Stress Tensor Using Earthquake Focal Mechanism Data – Application to the San-Fernando Earthquake Sequence. *J. Geophysics Res*. **89** (9), 305–9,320.

Jost, M.L. and Herrmann., R.B. [1989]. A Student's Guide to and Review of Moment Tensors. *Seismological Research Letters*. **60** (2), 37–57.

Michael, A.J. [1984]. Determination of Stress from Slip Data: Faults and Folds. *J. Geophys. Res*. **89,** 11,517–11,526.

Neuhaus, C.W., Williams, S., Remington, C., William, B.B., Blair, K., Neshyba, G. and McCay, T. [2012]. Integrated Microseismic Monitoring for Field Optimization in the Marcellus Shale – A Case Study. *SPE Canadian Unconventional Resources Conference,* Extended Abstracts.

Reches, Z. [1987]. Determination of the tectonic stress tensor from slip analysis along faults that obey the coulomb yield condition. *Tectonics*, **6** (6), 849-861.

Sasaki, S. and Kaieda, H. [2002]. Determination of Stress State from Focal Mechanisms of Microseismic Events Induced During Hydraulic Injection at the Hijiori Hot Dry Rock Site. *Pure Appl. Geophys.,* **159**, 489–516.

Stanek, F., Jechumtalova, Z. and Eisner, L. [2015]. Reservoir stress from microseismic source mechanisms*, The Leading Edge*, **34**, (8), 76-78.

Zoback, M.D. [2010]. *Reservoir Geomechanics*. (1st Edition), Cambridge University Press, New York, USA.